LETTERS

p53 and Pten control neural and glioma stem/progenitor cell renewal and differentiation

Hongwu Zheng[1]*, Haoqiang Ying[1]*, Haiyan Yan[1], Alec C. Kimmelman[1,4], David J. Hiller[8], An-Jou Chen[1], Samuel R. Perry[1,2], Giovanni Tonon[1], Gerald C. Chu[1,2,5], Zhihu Ding[1], Jayne M. Stommel[1], Katherine L. Dunn[1], Ruprecht Wiedemeyer[1], Mingjian J. You[1], Cameron Brennan[9,10], Y. Alan Wang[1,2], Keith L. Ligon[1,3,5,6], Wing H. Wong[8], Lynda Chin[1,2,7] & Ronald A. DePinho[1,2,11]

Glioblastoma (GBM) is a highly lethal brain tumour presenting as one of two subtypes with distinct clinical histories and molecular profiles. The primary GBM subtype presents acutely as a high-grade disease that typically harbours mutations in *EGFR, PTEN* and *INK4A/ARF* (also known as *CDKN2A*), and the secondary GBM subtype evolves from the slow progression of a low-grade disease that classically possesses *PDGF* and *TP53* events[1–3]. Here we show that concomitant central nervous system (CNS)-specific deletion of *p53* and *Pten* in the mouse CNS generates a penetrant acute-onset high-grade malignant glioma phenotype with notable clinical, pathological and molecular resemblance to primary GBM in humans. This genetic observation prompted *TP53* and *PTEN* mutational analysis in human primary GBM, demonstrating unexpectedly frequent inactivating mutations of *TP53* as well as the expected *PTEN* mutations. Integrated transcriptomic profiling, *in silico* promoter analysis and functional studies of murine neural stem cells (NSCs) established that dual, but not singular, inactivation of *p53* and *Pten* promotes an undifferentiated state with high renewal potential and drives increased Myc protein levels and its associated signature. Functional studies validated increased Myc activity as a potent contributor to the impaired differentiation and enhanced renewal of NSCs doubly null for *p53* and *Pten* ($p53^{-/-}$ $Pten^{-/-}$) as well as tumour neurospheres (TNSs) derived from this model. Myc also serves to maintain robust tumorigenic potential of $p53^{-/-}$ $Pten^{-/-}$ TNSs. These murine modelling studies, together with confirmatory transcriptomic/promoter studies in human primary GBM, validate a pathogenetic role of a common tumour suppressor mutation profile in human primary GBM and establish Myc as an important target for cooperative actions of p53 and Pten in the regulation of normal and malignant stem/progenitor cell differentiation, self-renewal and tumorigenic potential.

High-grade malignant glioma, the most common intrinsic brain tumour, is uniformly fatal despite maximum treatment[3]. A wealth of molecular genetic studies has established central roles of the RTK-PI3K-PTEN, ARF-MDM2-p53 and INK4a-RB pathways in gliomagenesis[3,4]. To explore the role of p53 and Pten in glioma, we used the *hGFAP-Cre* transgene[5,6] to delete *p53* alone or in combination with *Pten* in all CNS lineages using conditional *p53* (ref. 7) and *Pten* alleles (Supplementary Figs 1 and 2a–c). Because broad CNS deletion of *Pten* results in lethal hydrocephalus in early postnatal life (data not shown), modelling efforts henceforth emphasized the $Pten^{lox/+}$ genotype.

Clinically, between 15 to 40 weeks of ages, 42 out of 57 (73%) of the $hGFAP\text{-}Cre^{+};p53^{lox/lox};Pten^{lox/+}$ mice presented with acute-onset neurological symptoms—seizure, ataxia and/or paralysis (Fig. 1a). Histopathologically, all 42 neurologically symptomatic mice harboured malignant gliomas that were classified on the basis of WHO (World Health Organization) criteria[8] as anaplastic astrocytomas (WHO III, $n = 28$, 66%) or GBM (WHO IV, $n = 14$, 34%; Fig. 1b). These GBMs had classical features of pseudopalisading necrosis, marked cellular pleomorphism, and highly infiltrative spread including perineuronal and perivascular satellitosis as well as subpial spread in the cerebral cortex (Supplementary Fig. 3a). Occasionally tumours had abnormal vessels suggestive of microvascular proliferation. All tumours showed increased mitoses (Ki67 staining) and expression of the classical human glioma markers Gfap and Nestin (Fig. 1c). Necropsy of 15 neurologically asymptomatic mice showed no cases of incipient low-grade glioma disease but 8 had high-grade pathology including very small lesions with anaplastic features of nuclear atypia, multinucleated tumour cells and/or high cellularity (Supplementary Fig. 3b). For the remaining genotypes, 4 out of 23 $hGFAP\text{-}Cre^{+};p53^{lox/lox}$ mice developed anaplastic astrocytoma (WHO III); conversely 19 out of 23 $hGFAP\text{-}Cre^{+};p53^{lox/lox}$ mice, 12 out of 12 $hGFAP\text{-}Cre^{+};p53^{lox/+};Pten^{lox/+}$ mice and 10 out of 10 $hGFAP\text{-}Cre^{+};p53^{lox/+}$ mice had no CNS pathology and developed only non-CNS tumours (data not shown).

Historically, *TP53* inactivation has been considered a classical lesion in low-grade astrocytomas and secondary GBM but infrequently in primary GBM[1,9]. The remarkable clinical and histological resemblance of this model to the primary GBM subtype in humans prompted *TP53* and *PTEN* resequencing in human primary GBM. Of the 35 clinically annotated human primary GBM samples, 10 (29%) tumours registered prototypical *TP53* mutations and 14 (40%) tumours had *PTEN* missense mutations, insertions, deletions or splicing mutations (Supplementary Table 1). Moreover, six out of ten tumours with *TP53* mutations harboured concomitant *PTEN* mutations or homozygous deletion. Encouragingly, our mutational data agrees with The Cancer Genome Atlas data reporting *TP53* and *PTEN* as the two most commonly mutated tumour suppressor genes (http://tcga-data.nci.nih.gov/tcga/findArchives.htm). These results, together with recent population-based studies[10,11], indicate that *TP53* is a key tumour suppressor for both GBM subtypes.

Consistent with frequent *PTEN* loss of heterozygosity (LOH; 60–70%) in human high-grade glioma[3], 16 out of 16 mouse high-grade

[1]Department of Medical Oncology, [2]Center for Applied Cancer Science, Belfer Foundation Institute for Innovative Cancer Science, [3]Center for Molecular Oncologic Pathology, Dana-Farber Cancer Institute and Harvard Medical School, Boston, Massachusetts 02115, USA. [4]Harvard Radiation Oncology Program, [5]Department of Pathology, [6]Division of Neuropathology, [7]Department of Dermatology, Brigham and Women's Hospital, Harvard Medical School, Boston, Massachusetts 02115, USA. [8]Department of Statistics, Stanford University, Stanford, California 94305, USA. [9]Department of Neurosurgery, Memorial Sloan-Kettering Cancer Center, New York, New York 10065, USA. [10]Department of Neurosurgery, Weill-Cornell Medical College, New York, New York 10065, USA. [11]Departments of Medicine and Genetics, Harvard Medical School, Boston, Massachusetts 02115, USA. *These authors contributed equally to this work.

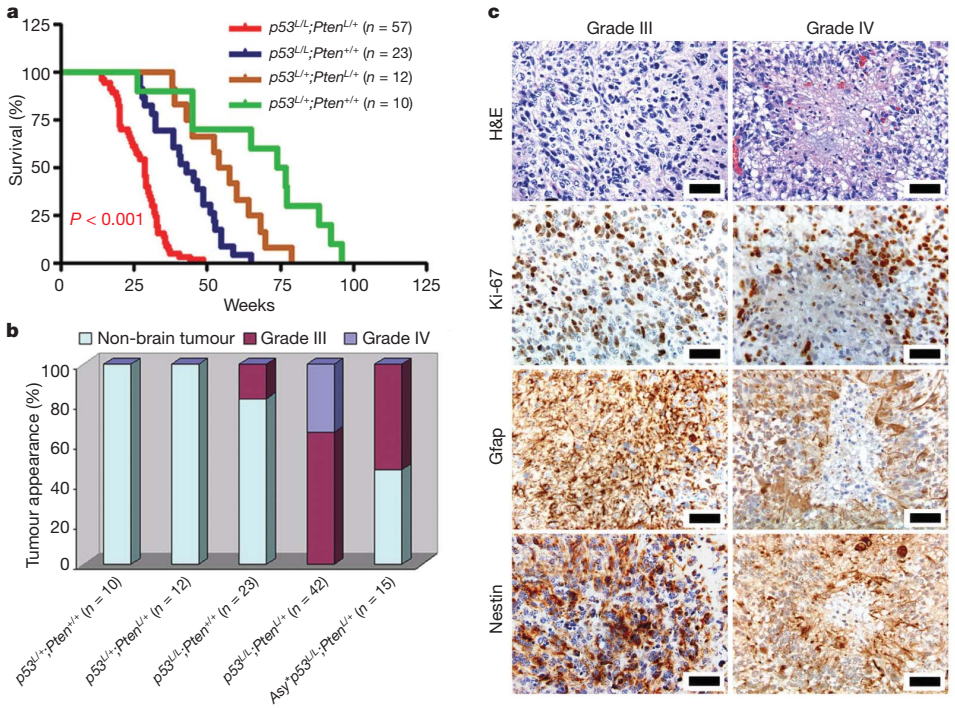

Figure 1 | *p53* and *Pten* inactivation cooperate to induce high-grade malignant gliomas. a, Kaplan–Meier tumour-free survival curves for mice of indicated genotypes as a function of weeks. '+' designates the wild-type allele, '*L*' denotes the conditional allele. **b**, Graph shows frequency and grade of gliomas versus non-CNS malignancies observed in end-stage of indicated mice from **a**. *Asy** indicates neurological asymptomatic *hGFAP-Cre*$^{+}$;*p53*$^{lox/lox}$;*Pten*$^{lox/+}$ mice ($n = 15$) killed for non-CNS malignancies. **c**, Haematoxylin and eosin (H&E) histology and immunohistochemical staining of sections of WHO grade III and IV malignant gliomas from *hGFAP-Cre*$^{+}$;*p53*$^{lox/lox}$;*Pten*$^{lox/+}$ mice with antibodies against Ki67, Gfap and Nestin. Scale bars, 50 μm.

gliomas showed no Pten expression in tumour cells but a robust signal in surrounding non-malignant cells and intratumoral vessels (Fig. 2a). Polymerase chain reaction (PCR) genotyping indicated that six out of seven tested tumours sustained loss of the wild-type *Pten* allele (Fig. 2b). The *Pten* reduction to homozygosity and the documented Cre-mediated deletion of both *p53* floxed alleles indicate that the inactivation of both genes is required for gliomagenesis. Loss of Pten expression correlated with activation of key PI3K signalling surrogates: Akt and ribosomal protein S6 kinase (Fig. 2c). In accordance with human high-grade disease, eight out of eight malignant murine gliomas expressed high Vegf levels relative to normal brain tissue (Fig. 2c). Co-activation of multiple receptor tyrosine kinases in human primary GBM[12] was also evident in the murine tumours with robust Pdgfα expression overlapping with strong regional activation of Egfr (Supplementary Fig. 4a–d).

A classical feature of human high-grade malignant glioma is a significant degree of intertumoral and intratumoral morphological and lineage heterogeneity, hence the moniker glioblastoma 'mutliforme'. This characteristic plasticity was evident in the *hGFAP-Cre*$^{+}$;*p53*$^{lox/lox}$;*Pten*$^{lox/+}$ gliomas in which occasional tumours (5 out of 50) presented with both astrocytic and oligodendroglial histopathological features (Supplementary Fig. 5). The basis for morphological variability is not known and may relate, among many possibilities, to the acquisition of an immature developmental state with multipotency and/or differentiative plasticity. Consistent with this notion, all murine tumours express stem or lineage progenitor markers (including Nestin, Gfap and Olig2) similar to human glioma profiles[13] but are negative for mature neuronal and oligodendrocyte markers (NeuN and Mbp; Supplementary Fig. 6a, b). This stem/progenitor marker profile is in accord with the ability of all murine tumours tested to readily generate TNSs with (i) strong tumour-initiating potential with secondary tumours faithfully retaining the primary tumour's histological features (Supplementary Fig. 7); (ii) robust NSC marker Nestin expression; and (iii) limited capacity to differentiate into astrocytic and neuronal lineages after exposure to differentiation agents (Fig. 2d). As NSC/progenitor cells have been proposed to be the preferred cell-of-origin for GBM[6], the immature marker profile and varied morphological presentation of our murine tumours prompted us to posit that *Pten* and *p53* deficiencies might contribute to gliomagenesis by affecting NSC self-renewal and differentiation potential.

To explore this hypothesis, we characterized primary murine embryonic day (E)13.5 NSC cultures singly or doubly null for *p53* and *Pten*. Compared to NSCs null for either *Pten* or *p53*, which show only modestly increased proliferation and self-renewal reflected by neurosphere formation capacity[14–16], NSCs null for both *p53* and *Pten* showed significant proliferation and self-renewal activity (Fig. 3a and Supplementary Fig. 8a). This effect on NSC renewal, coupled with the aforementioned varied tumour histology, suggests that combined *p53* and *Pten* loss might cooperate in tumorigenesis by impairing NSC differentiation potential. When NSCs were continuously cultured in NSC medium, all genotypes showed a similar robust expression of NSC/progenitor markers (for example Nestin) and minimal expression of differentiated lineage markers (Supplementary Fig. 8b). After exposure to differentiation-inducing medium, wild-type and single-null NSC cultures differentiated into Gfap-positive astrocytes, Tuj1-positive neurons, or O4-positive oligodendrocytes. In contrast, *p53*$^{-/-}$ *Pten*$^{-/-}$ NSCs failed to respond to these differentiation cues and retained stem-cell-like morphology and lineage marker (Nestin) expression (Fig. 3b and Supplementary Fig. 9a). Similar

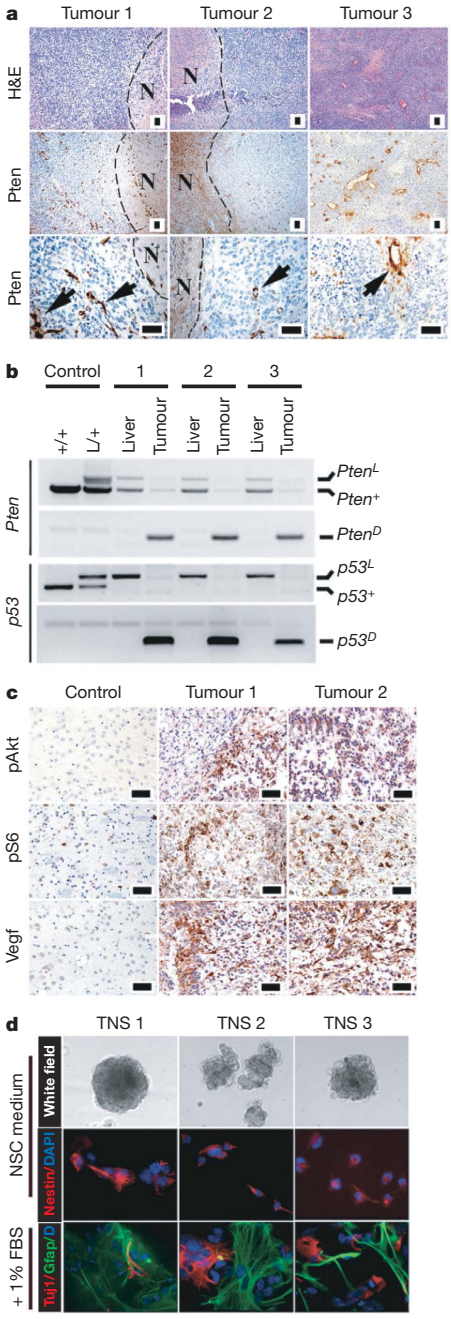

Figure 2 | *hGFAP-Cre*$^{+}$*;p53*$^{lox/lox}$*;Pten*$^{lox/+}$ gliomas mirror key features of human malignant gliomas. **a**, Pten expression is completely extinguished in tumour cells. Sections of three independent malignant gliomas were stained with haematoxylin and eosin (H&E) and an anti-Pten antibody. 'N' indicates the adjacent normal regions of the tumour cells; the arrows point to Pten-positive vascular cells embedded in the tumour. **b**, The wild-type *Pten* allele is lost in glioma cells. Genomic DNA isolated from liver tissues and brain tumour cells was subjected to PCR-based assays for genotyping *Pten* and *p53* alleles. '+' designates the *Pten* wild-type allele, '*L*' denotes the conditional allele, and '*D*' denotes the inactivated form of the conditional allele after Cre-mediated recombination. **c**, Immunohistochemical staining of mouse normal brain or glioma sections with antibodies against activated phosphorylated Akt (pAkt), phosphorylated ribosomal protein S6 kinase (pS6) and Vegf. **d**, TNS lines isolated from independent malignant gliomas were cultured in NSC medium or differentiation medium (1% fetal bovine serum (FBS)) and immunostained for Nestin, Gfap and Tuj1 as indicated. Scale bars, 50 μm (**a**, **c**); original magnification in **d** ×400.

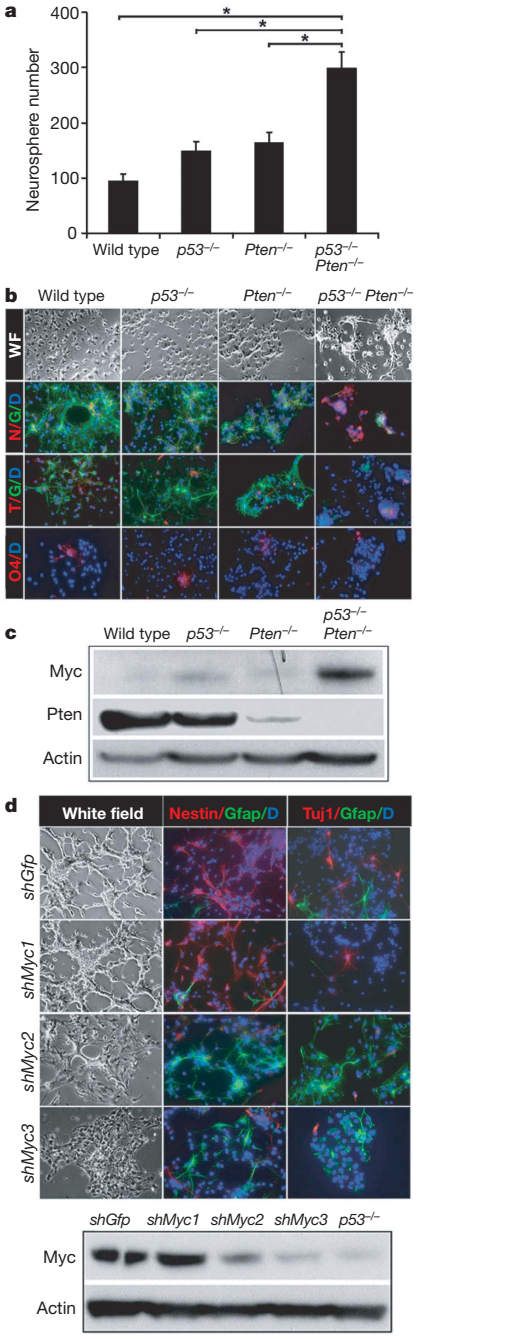

Figure 3 | *p53* and *Pten* coordinately regulate Myc protein level as well as NSC self-renewal and differentiation. **a**, The number of neurospheres formed by $p53^{-/-}$ $Pten^{-/-}$ NSCs in culture is significantly increased as compared to wild-type or singly null NSCs; asterisk, $P < 0.001$; $n = 3$. Values represent mean ± s.d. from three experiments. **b**, The multilineage differentiation potential was impaired in $p53^{-/-}$ $Pten^{-/-}$ NSCs. D, DAPI (blue); G, Gfap (green); N, Nestin (red); O4 (red); WF, white field; T, Tuj-1 (red). **c**, Combined inactivation of *p53* and *Pten* in NSCs stimulates Myc protein expression. **d**, Knockdown of Myc expression restores $p53^{-/-}$ $Pten^{-/-}$ NSC differentiation capacity. Lower panel, western blot of double-null NSC Myc protein expression after infected with indicated lentiviral shRNA. Note Myc expression in *shMyc2-* and *shMyc3*-infected $p53^{-/-}$ $Pten^{-/-}$ cells is comparable to that in $p53^{-/-}$ cells, and *shMyc1* as a control shows no knockdown. Original magnification used for **b** and **d**: ×200.

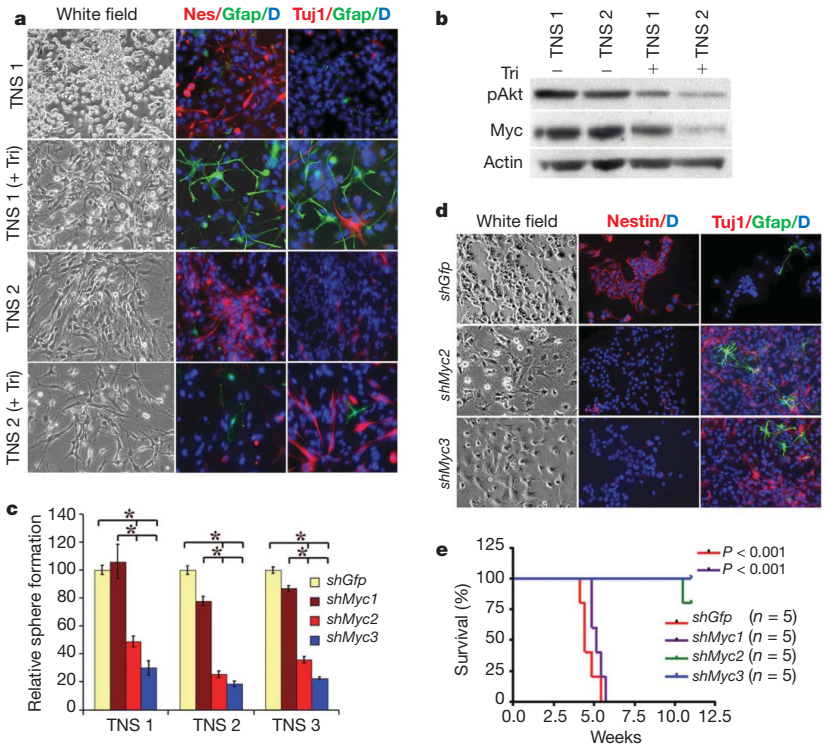

Figure 4 | Attenuated Myc expression restores *hGFAP-Cre^{+};p53$^{lox/lox}$;Pten$^{lox/+}$* TNS differentiation potential and reduces tumorigenic potential. a, Inhibition of the Akt pathway by triciribine induces TNS cell differentiation. Two independent TNS lines were cultured in 1% FBS in the absence or presence of triciribine (Tri, 5 μM) for 7 days before being subjected to immunostaining with antibodies against Nestin (Nes, red), Gfap (Green) and Tuj1 (red). D, DAPI (blue). **b**, Inhibition of the Akt pathway in TNS cells with triciribine attenuates their cellular Myc expression. **c**, Knockdown of Myc expression in TNS cells reduces their self-renewal potential assessed by sphere formation; asterisk, $P < 0.001$; $n = 3$. Values represent mean ± s.d. from three experiments. **d**, shRNA-mediated reduction of Myc expression in TNS cells sensitizes cells to differentiation stimuli. Cells infected with control (*shGfp*) and the indicated shRNA were incubated with differentiation medium before being subjected to lineage marker analysis. **e**, shRNA-mediated reduction of Myc expression represses TNS tumorigenic potency in orthotopically transplanted SCID mice. Original magnification for **a** and **d**: ×200.

differentiation defect and abnormal self-renewal potential were also observed in adult NSCs that were deleted for *Pten* and *p53* postnatally (Supplementary Fig. 9b, c). The contribution of *Pten* deficiency in maintaining impaired differentiation was further verified by the ability of the Akt inhibitor triciribine[17] to enable differentiation of NSCs null for both *Pten* and *p53* (Supplementary Fig. 10a, b).

To understand the molecular basis of impaired differentiation capacity, we performed transcriptome comparisons of murine $p53^{-/-}$ NSCs with $p53^{-/-}$ $Pten^{-/-}$ NSCs at 1 day after exposure to the differentiation inducer. Among the 410 genes showing significant differential expression (Supplementary Table 2) promoter analysis identified E2F and Myc motifs as two of the most enriched promoter binding elements (1.7× and 1.4×, respectively; $P < 10^{-4}$). Notably, promoter analysis using 69 pretreatment human primary GBM cases in the TCGA database showed strong enrichment of MYC binding elements: 10 $p53^{-/-}$ $Pten^{-/-}$ double-mutant tumours versus the 59 remaining tumours (1.40×, $P = 2.20 \times 10^{-3}$) or versus the 12 $p53^{-/-}$ single-mutant tumours (1.46×, $P = 1.54 \times 10^{-3}$).

MYC is well-known for its roles in cell cycle progression and apoptosis[18] as well as in stem cell self-renewal and differentiation during development and oncogenic processes[19–22]. It is also notable that both p53 and Pten/PI3K pathways can directly regulate MYC with p53 repressing *MYC* transcription by directly binding to the *MYC* promoter[23], whereas downstream PI3K pathway arms can modulate MYC translation and protein degradation[24,25]. In agreement, Myc protein levels were substantially increased in the murine double-null NSCs, but only marginally elevated in $p53^{-/-}$ or $Pten^{-/-}$ NSCs when compared to wild-type controls (Fig. 3c), raising the possibility that p53 and Pten cooperate to regulate Myc levels which in turn could control NSC self-renewal and differentiation.

To test this hypothesis, we examined the effect of Myc knockdown on murine $p53^{-/-}$ $Pten^{-/-}$ NSC differentiation potential and observed that Myc short hairpin RNA (shRNA; *shcMyc2* and *shcMyc3*), which reduced Myc levels to those in $p53^{-/-}$ NSCs, largely restored their differentiation capacity (Fig. 3d and Supplementary Fig. 11a). Conversely, enforced Myc expression in $p53^{-/-}$ NSCs repressed their differentiation and enabled retention of stem/progenitor marker expression (Nestin and Sox2; Supplementary Fig. 11b), indicating that the concomitant loss of p53 and Pten elevates Myc activity to impede NSC differentiation capacity.

The strong pleiotropic activities attributed to MYC demands tight control of its expression to avoid development of diverse human malignancies, including gliomas[21,26]. Our finding that the concomitant loss of p53 and Pten compromises NSC differentiation capacity by means of elevated Myc levels prompted further assessment of its relevance in the so-called 'brain cancer stem cells' in our model. Using murine TNSs which are enriched for such tumour initiating cells (TICs), Akt inhibitor treatment strongly reduced Myc protein and promoted differentiation (Fig. 4a, b and Supplementary Fig. 12a). Correspondingly, Myc knockdown in TNS cells not only markedly reduced their proliferation and self-renewal capacity (Fig. 4c and Supplementary Fig. 12b, c) but also strongly sensitized them to differentiation induction (Fig. 4d and Supplementary Fig. 12d). Notably, although ten out of ten intracranial injections of vector-transduced murine TNSs resulted in lethal infiltrating gliomas within 1 month, nine out of ten mice injected with Myc knockdown TNSs

survived for more than 3 months (Fig. 4e). Thus, Myc has a crucial involvement in maintaining the impaired differentiation and potent tumorigenic potential of *p53*- and *Pten*-inactive TNSs (Supplementary Fig. 13).

The identification of TICs with stem-like properties in diverse human cancers including GBM represents an important conceptual advance in cancer biology with therapeutic implications[27,28]. These TICs seem to constitute a reservoir of self-sustaining cells with potent tumorigenic potential. However, unlike normal NSCs which readily differentiate along a developmental hierarchy into lineage-restricted differentiated progenies, TNSs derived from $p53^{-/-}$ $Pten^{-/-}$ malignant gliomas show resistance towards differentiation cues. The diminished tumorigenicity of these TICs on restoration of differentiation potential, along with recent reports supporting pro-differentiation as a potential strategy to inhibit GBM-derived TICs[29,30], encourages the identification and testing of agents targeting these differentiation pathways including MYC in the treatment of primary GBM in humans.

METHODS SUMMARY

Standard gene targeting and chimaera formation methods were used to generate the conditional $Pten^{L}$ allele in the mouse germ line in which *Pten* exon 5 is flanked by loxP sites; the conditional $p53^{L}$ mouse was generated by A. Berns; *hGFAP-Cre* mice were purchased from the Jackson Laboratory. All mice were maintained in pathogen-free facilities and followed for development of neurological deficits. After culling, tissues were collected and processed for histological, immunohistochemical, immunofluorescence or western blot analyses, as detailed in the Methods. For *p53* and *Pten* mutation analysis, surgically resected human primary glioblastoma were flash-frozen and genomic DNA was prepared from frozen tumour samples. For microarray analysis, total RNAs from indicated early passage NSCs were amplified and labelled by standard methods and hybridized to Affymetrix 430 2.0 chips. For tumorigenic analysis, TNS cells isolated from $hGFAP\text{-}Cre^{+};p53^{lox/lox};Pten^{lox/+}$ murine malignant gliomas were infected with indicated lentivirus shRNA and orthotopically injected into the forebrain of SCID mice. Animals were observed daily for the development of neurological deficits and subjected to histological analysis once killed.

Full Methods and any associated references are available in the online version of the paper at www.nature.com/nature.

Received 2 May; accepted 10 September 2008.

1. Kleihues, P. & Ohgaki, H. Primary and secondary glioblastomas: from concept to clinical diagnosis. *Neuro-oncol.* **1,** 44–51 (1999).
2. Zhu, Y. & Parada, L. F. The molecular and genetic basis of neurological tumours. *Nature Rev. Cancer* **2,** 616–626 (2002).
3. Furnari, F. B. *et al.* Malignant astrocytic glioma: genetics, biology, and paths to treatment. *Genes Dev.* **21,** 2683–2710 (2007).
4. Wiedemeyer, R. *et al.* Feedback circuit among INK4 tumor suppressors constrains human glioblastoma development. *Cancer Cell* **13,** 355–364 (2008).
5. Zhuo, L. *et al.* hGFAP-cre transgenic mice for manipulation of glial and neuronal function *in vivo*. *Genesis* **31,** 85–94 (2001).
6. Zhu, Y. *et al.* Early inactivation of p53 tumor suppressor gene cooperating with NF1 loss induces malignant astrocytoma. *Cancer Cell* **8,** 119–130 (2005).
7. Jonkers, J. *et al.* Synergistic tumor suppressor activity of BRCA2 and p53 in a conditional mouse model for breast cancer. *Nature Genet.* **29,** 418–425 (2001).
8. Louis, D. N., Ohgaki, H., Wiestler, O. D. & Cavenee, W. K. *WHO Classification of Tumours of the Central Nervous System* 4th edn (eds Louis, D. N., Ohgaki, H., Wiestler, O.D. & Cavenee, W.K.) (World Health Organization, 2007).
9. Watanabe, K. *et al.* Overexpression of the EGF receptor and p53 mutations are mutually exclusive in the evolution of primary and secondary glioblastomas. *Brain Pathol.* **6,** 217–223 (1996).
10. Ohgaki, H. *et al.* Genetic pathways to glioblastoma: a population-based study. *Cancer Res.* **64,** 6892–6899 (2004).
11. Fukushima, T. *et al.* Genetic alterations in primary glioblastomas in Japan. *J. Neuropathol. Exp. Neurol.* **65,** 12–18 (2006).
12. Stommel, J. M. *et al.* Coactivation of receptor tyrosine kinases affects the response of tumor cells to targeted therapies. *Science* **318,** 287–290 (2007).
13. Ligon, K. L. *et al.* Olig2-regulated lineage-restricted pathway controls replication competence in neural stem cells and malignant glioma. *Neuron* **53,** 503–517 (2007).
14. Groszer, M. *et al.* PTEN negatively regulates neural stem cell self-renewal by modulating G_0–G_1 cell cycle entry. *Proc. Natl Acad. Sci. USA* **103,** 111–116 (2006).
15. Gil-Perotin, S. *et al.* Loss of p53 induces changes in the behavior of subventricular zone cells: implication for the genesis of glial tumors. *J. Neurosci.* **26,** 1107–1116 (2006).
16. Meletis, K. *et al. p53* suppresses the self-renewal of adult neural stem cells. *Development* **133,** 363–369 (2006).
17. Yang, L. *et al.* Akt/protein kinase B signaling inhibitor-2, a selective small molecule inhibitor of Akt signaling with antitumor activity in cancer cells overexpressing Akt. *Cancer Res.* **64,** 4394–4399 (2004).
18. Patel, J. H., Loboda, A. P., Showe, M. K., Showe, L. C. & McMahon, S. B. Analysis of genomic targets reveals complex functions of MYC. *Nature Rev. Cancer* **4,** 562–568 (2004).
19. Cartwright, P. *et al.* LIF/STAT3 controls ES cell self-renewal and pluripotency by a Myc-dependent mechanism. *Development* **132,** 885–896 (2005).
20. Takahashi, K. & Yamanaka, S. Induction of pluripotent stem cells from mouse embryonic and adult fibroblast cultures by defined factors. *Cell* **126,** 663–676 (2006).
21. Ben-Porath, I. *et al.* An embryonic stem cell-like gene expression signature in poorly differentiated aggressive human tumors. *Nature Genet.* **40,** 499–507 (2008).
22. Wong, D. J. *et al.* Module map of stem cell genes guides creation of epithelial cancer stem cells. *Cell Stem Cell* **2,** 333–344 (2008).
23. Ho, J. S., Ma, W., Mao, D. Y. & Benchimol, S. p53-Dependent transcriptional repression of c-myc is required for G_1 cell cycle arrest. *Mol. Cell. Biol.* **25,** 7423–7431 (2005).
24. Gera, J. F. *et al.* AKT activity determines sensitivity to mammalian target of rapamycin (mTOR) inhibitors by regulating cyclin D1 and c-*myc* expression. *J. Biol. Chem.* **279,** 2737–2746 (2004).
25. Sears, R. *et al.* Multiple Ras-dependent phosphorylation pathways regulate Myc protein stability. *Genes Dev.* **14,** 2501–2514 (2000).
26. Bredel, M. *et al.* Functional network analysis reveals extended gliomagenesis pathway maps and three novel MYC-interacting genes in human gliomas. *Cancer Res.* **65,** 8679–8689 (2005).
27. Clarke, M. F. *et al.* Cancer stem cells–perspectives on current status and future directions: AACR Workshop on cancer stem cells. *Cancer Res.* **66,** 9339–9344 (2006).
28. Lobo, N. A., Shimono, Y., Qian, D. & Clarke, M. F. The biology of cancer stem cells. *Annu. Rev. Cell Dev. Biol.* **23,** 675–699 (2007).
29. Piccirillo, S. G. *et al.* Bone morphogenetic proteins inhibit the tumorigenic potential of human brain tumour-initiating cells. *Nature* **444,** 761–765 (2006).
30. Lee, J. *et al.* Epigenetic-mediated dysfunction of the bone morphogenetic protein pathway inhibits differentiation of glioblastoma-initiating cells. *Cancer Cell* **13,** 69–80 (2008).

Supplementary Information is linked to the online version of the paper at www.nature.com/nature.

Acknowledgements We thank A. Berns for providing $p53^{L}$ mice; S. Zhou and S. Jiang for mouse husbandry and care; R. T. Bronson for discussion on pathology analysis; K. Montgomery for discussion on sequencing; and Y.-H. Xiao, B. Feng and J. Zhang for bioinformatic help. H.Z. was supported by Helen Hay Whitney Foundation. H. Ying is a recipient of the Marsha Mae Moeslein Fellowship from the American Brain Tumor Association. A.C.K. is a recipient of the Leonard B. Holman Research Pathway Fellowship. Z.D. is supported by the Damon Runyon Cancer Research Foundation. J.M.S. is supported by a Ruth L. Kirschstein National Research Service Award Fellowship. R.W. is supported by a Mildred Scheel Fellowship (Deutsche Krebshilfe). Grant support comes from the Goldhirsh Foundation (R.A.D.), and NIH grants U01 CA84313 (R.A.D.), RO1CA99041 (L.C.) and 5P01CA95616 (R.A.D., L.C., W.H.W., C.B. and K.L.L.). R.A.D. is an American Cancer Society Research Professor supported by the Robert A. and Renee E. Belfer Foundation Institute for Innovative Cancer Science.

Author Contributions H.Z. and H. Ying performed the experiments and contributed equally as first authors. R.A.D. supervised experiments and contributed as senior author. M.J.Y. generated the $Pten^{L}$ mouse allele. D.J.H., W.H.W. and G.T. conducted the microarray and promoter analyses. K.L.L., H.Z. and G.C.C. provided the pathology analyses. H. Yan, A.C.K., A.-J.C., S.R.P., Z.D., J.M.S, K.L.D. and R.W. performed the experiments. C.B. contributed patient samples and pathologic information. L.C. and Y.A.W. contributed to the writing of the manuscript.

Author Information Reprints and permissions information is available at www.nature.com/reprints. Correspondence and requests for materials should be addressed to R.A.D. (ron_depinho@dfci.harvard.edu).

METHODS

Mice. *p53*^{L} and *hGFAP-Cre* mice have been described previously[5,7]. *Pten*^{L} mice were generated using a standard knock-in approach in which *Pten* exon 5 is flanked by loxP sites (details on targeting construct and procedures are available on request). Mice were interbred and maintained on a FvB/C57Bl6 hybrid background in pathogen-free conditions at the Dana-Farber Cancer Institute, monitored for signs of ill-health every other day, and euthanized and necropsied when moribund. All manipulations were performed with Institutional Animal Care and Use Committee (IACUC) approval.

Histology and immunohistochemistry. Once killed, mice were perfused with 4% paraformaldehyde (PFA) and brains were dissected, followed by overnight post-fixation in 4% PFA at 4 °C. Serial sections were prepared at 5 μm for paraffin sections or 10 μm for cryostat sections with every tenth slide stained by haematoxylin and eosin (DF/HCC Research Pathology Cores). Tumour grading was determined by K.L.L. and H.Z. on the basis of the WHO grading system for malignant astrocytoma[8]. Immunohistochemical and immunofluorescence analyses were performed as described[31]. The Pdgfrα and pEgfr double immunohistochemical staining was performed using DakoCytomation EnVision doublestain system (K1395, Dako) following manufacturer's instructions. The primary antibodies used were: Ki67 (VP-RM04, Vector), Gfap (Z0334, DAKO), Gfap (556330, BD Pharmingen), Nestin (MAB353, Chemicon; specifically for mouse), Nestin (MAB5326, Chemicon; specifically for human), Pten (9559, Cell Signaling), phospho-Akt^{Ser473} (3787, Cell Signaling), phospho-ribosomal protein S6 kinase (2215, Cell Signaling), Cyclin D1 (18-0220, ZYMED), Vegf (sc-152, Santa Cruz), Pdgfrα (3174, Cell Signaling), phospho-Pdgfrα^{Y754} (sc-12911, Santa Cruz), Egfr (IHC-00005, Bethyl), phospho-Egfr^{Y1068} (ab40815, Abcam), phospho-Egfr^{Y1173} (sc-12351, Santa Cruz), Olig-2 (AB9610, Chemicon), Tuj-1 (MMS-435P, Covance), O4 (MAB1326, R&D), NeuN (MAB377, Millipore), Mbp (ab7349, Abcam), Myc (ab39688, Abcam), and Cre (69050-3, Novagen). Images were captured using a Leica DM1400B microsystem and Leica FW4000 version 1.2.1.

Cell culture. Primary NSCs were isolated from the brain subventricular zone (SVZ) of E13.5 embryos or 1-month-old mice with the indicated genotype as previously described[31,32]. NSCs were maintained in NSC proliferation media (05702, StemCell) supplemented with 20 ng ml^{-1} EGF (E4127, Sigma) and 10 ng ml^{-1} bFGF (F0291, Sigma). To generate primary TNS cells, tumour samples from freshly dissected mouse brains were subjected to mechanical and enzymatic dissociation. Single-cell suspensions were cultured in NSC proliferation media. Tumour spheres formed were then disaggregated and used for indicated assays. NSC differentiation assays were carried out by plating the indicated cells in culture wells on coverslips precoated with 15 μg ml^{-1} poly-l-ornithine (P3655, Sigma) and 1 μg ml^{-1} fibronectin (F1141, Sigma); the cells were incubated in neurobasal medium supplemented with 1% FBS for 7–10 days, and the differentiation capacities were examined under either a light or fluorescence microscope (Nikon). For TNS cell differentiation, cells were incubated in differentiation media with varying doses of triciribine (BioMol) or vehicle (dimethylsulphoxide, Sigma). Knockdown of mouse Myc was performed by infecting the indicated cells with lentivirus containing *shMyc* constructs (provided by W. Hahn). The shRNA constructs *shMyc1*, *shMyc2* and *shMyc3* correspond to clone IDs TRCN000000 54856, 42517 and 42513, respectively (The DFCI-Broad RNAi Consortium, commercially available from Sigma-Aldrich).

Western, cell growth and self-renewal assays. Western blot assays were performed as previously described[31] with antibodies against Myc (sc-42, Santa Cruz), phospho-Akt^{Ser473} (9271, Cell Signaling), Pten (9569, Cell Signaling) and Actin (sc-1615, Santa Cruz). For *in vitro* cell growth assays, NSCs or TNS cells (10,000) were plated in triplicate in 96-well format and incubated in NSC proliferation media for 5 days, and growth was quantified using Luminescence ATP detection assay system (PerkinElmer). Self-renewal capacity was measured by plating 1,000 cells per well (6-well plate) in NSC proliferation media containing EGF and bFGF with 0.3% agarose (A9049, Sigma). The number of neurospheres or tumour neurospheres that formed subsequently per well was quantified after 10–14 days and relative sphere formation was plotted versus indicated control. Three replicates were performed for each. All experiments were conducted at cell passage <5.

Orthotopic transplants. Female SCID mice (Charles River) aged 6–8 weeks were anesthetized and placed into stereotactic apparatus equipped with a *Z* axis (Stoelting). A small hole was bored in the skull 0.5 mm anterior and 3.0 mm lateral to the bregma using a dental drill. Twenty thousand cells in Hanks Buffered Salt Solution was injected into the right caudate nucleus 3 mm below the surface of the brain using a 10-μl Hamilton syringe with an unbeveled 30 gauge needle. The scalp was closed using a 9-mm Autoclip Applier. Animals were followed daily for the development of neurological deficits.

Mutation screening. Frozen tumour specimens were obtained from the Memorial Sloan Kettering Cancer Center tumour bank. Genomic DNA was prepared from frozen primary GBM tumour samples using the Qiagen genomic purification kit. Coding exons were PCR amplified and sequenced using standard protocols at the Harvard Partners Center for Genetics and Genomics as previously described[33]. All known single nucleotide polymorphisms and synonymous mutations were removed from the analysis in the current study. This study was approved by the Institutional Review Board of the hospital.

Microarray analysis. Early passage wild-type and indicated mutant NSCs were incubated with NSC proliferation media or differentiation media for 18 h. RNA was isolated using Trizol (Invitrogen) and the RNeasy mini kit (Qiagen). Gene expression profiling was performed using the Affymetrix 430 2.0 chips at DFCI Microarray core facility.

Promoter analysis. Gene expressions were modelled using dChip software[34]. Sets of genes differentially expressed pre- and post-differentiation induction were generated using the SAM statistic[35], with a cutoff of ±2.0. Promoter analysis on both these gene sets used the CisGenome software (http://biogibbs.stanford.edu/~jihk/CisGenome/index.htm) to scan the 8 kb upstream to 2 kb downstream regions of these genes for the ~550 motifs in the TRANSFAC 12.1 database. Enrichment was measured against control regions at a comparable distance from the transcription start sites of random genes.

Statistical analysis. Tumour-free survivals were analysed using Graphpad Prism4. Statistical analyses were performed using the non-parametric Mann–Whitney test. Significance of enrichment in the promoter analysis was computed based on Poisson distribution with Bonferroni correction. Comparisons of cell growth, self-renewal and differentiation were performed using the unpaired Student's *t*-test. For all experiments with error bars, standard deviation was calculated to indicate the variation within each experiment and data, and values represent mean ± s.d.

31. Bachoo, R. M. *et al.* Epidermal growth factor receptor and Ink4a/Arf: convergent mechanisms governing terminal differentiation and transformation along the neural stem cell to astrocyte axis. *Cancer Cell* **1**, 269–277 (2002).
32. Rietze, R. L. & Reynolds, B. A. Neural stem cell isolation and characterization. *Methods Enzymol.* **419**, 3–23 (2006).
33. Maser, R. S. *et al.* Chromosomally unstable mouse tumours have genomic alterations similar to diverse human cancers. *Nature* **447**, 966–971 (2007).
34. Li, C. & Wong, W. H. Model-based analysis of oligonucleotide arrays: expression index computation and outlier detection. *Proc. Natl Acad. Sci. USA* **98**, 31–36 (2001).
35. Tusher, V. G., Tibshirani, R. & Chu, G. Significance analysis of microarrays applied to the ionizing radiation response. *Proc. Natl Acad. Sci. USA* **98**, 5116–5121 (2001).